CIMAC CONGRESS 25
ZURICH, MAY 19 – 23, 2025

2025 | 071

A multi-scale fourier feature network for efficient lubrication analysis of engine rough surfaces

Tribology

yihu tang, SMDERI

Limin Wu, SMDERI
Gang Liang, SMDERI
Junqiang Hu, SMDERI
LiTing Li, SMDERI

ABSTRACT

The rapid and accurate analysis of flow characteristics on rough surfaces is crucial for the lubrication design of friction pairs such as engine piston rings and bearings. Current lubrication analysis for rough surfaces predominantly uses finite difference method (FDM) or finite element method (FEM) to solve the average Reynolds equation. These methods require finely discretized computational grids for real rough surfaces and necessitate calculations across different film thicknesses to obtain flow factors within the average Reynolds equation. This results in large-scale computations that are time-consuming, significantly hindering the efficiency of lubrication analysis for real rough surfaces.

In recent years, physics-informed neural networks (PINNs) have developed rapidly and have been applied to the analysis of hydrodynamic lubrication on smooth surfaces. However, due to the inherent spectral bias problem of PINNs, they cannot be effectively applied to the lubrication analysis of rough surfaces with high-frequency characteristics. To address this limitation, this paper proposes a multi-scale lubrication network architecture suitable for the analysis of rough surface lubrication. This approach introduces a Fourier feature network with learnable frequency parameters to adaptively learn the frequency characteristics of rough surfaces and applies it to the calculation of flow factors. This method enables real-time calculation of flow factors. Even when considering the time required for network training, the computation time is significantly reduced, effectively doubling the efficiency compared with traditional methods.

This innovative approach offers a promising solution for the lubrication analysis of real rough surfaces, essential for optimizing the performance and longevity of engine components. It paves the way for more accurate and faster design processes in the lubrication of friction pairs, enhancing the overall efficiency of engine lubrication design.

1 INTRODUCTION

Modern engine components are increasingly subjected to harsh conditions, including thinner lubricating films, higher temperatures, and reduced lubricant availability. As a result, the impact of surface topography on lubricated contacts, especially in components like bearings and piston rings, has become more significant[1]. The growing recognition of surface roughness has led to efforts aimed at designing optimized surface textures to improve the tribological performance of these components. However, simulating rough surfaces presents a challenge due to the large difference in scale between global contact dimensions and local surface features. To address this, numerical methods typically employ either deterministic or stochastic approaches [2].Deterministic methods refine the computational mesh to capture surface features at the microscale, directly incorporating roughness into the film thickness equation. While accurate, this approach becomes high computational cost for real rough surfaces due to the fine meshes required. Stochastic methods, such as the flow factor technique [3] and homogenization methods [4], offer more efficient solutions but sacrifice detailed local flow information.

To mitigate the computational challenges of multiscale problems, machine learning, particularly Physics-Informed Neural Networks (PINNs), has emerged as a promising alternative [5]. PINNs integrate physical laws directly into the network architecture, enabling the solution of partial differential equations (PDEs) while incorporating boundary and initial conditions into the loss function. Pioneering work by Raissi [6] demonstrated the power of PINNs in solving PDEs efficiently, leading to applications in lubrication problems. Subsequent studies [7-11] expanded the use of PINNs to solve Reynolds equations, predicting oil film pressure distributions and performing sensitivity analyses. However, most of these studies focused on smooth surfaces, ignoring the effects of roughness, which are critical for realistic lubrication analysis.

A major limitation of PINNs is the "spectral bias," which causes the network to favor low-frequency solutions, making it difficult to model high-frequency features such as those found in rough surfaces [12]. Researchers have explored strategies like input encoding in higher-dimensional feature spaces to improve the network's ability to capture multiscale features. Wang's work on multiscale Fourier feature networks showed promise in solving specific PDEs, but these methods rely on fixed-frequency embeddings [13], limiting their flexibility in handling rough surface lubrication problems.

This paper introduces a novel deep learning framework to address these challenges. The method incorporates trainable frequency parameters in Fourier feature embeddings, enabling the network to dynamically adjust and select appropriate frequencies. This approach enhances the flexibility of the model, allowing it to effectively solve lubrication problems involving surface roughness. The proposed method is validated by comparing it with traditional FEM approaches, showing high consistency and significantly reduced computation times. This innovation not only addresses the spectral bias issue but also offers a more efficient solution for lubrication analysis in engineering applications.

2 HYDRODYNAMIC LUBRICATION

The Reynolds equation is commonly used to analyze textured or rough surfaces in hydrodynamic lubrication. This study employs the Multiscale lubrication Neural Network (MLNN) method, using a slider bearing as a case study to illustrate the hydrodynamic lubrication analysis of rough surfaces, as shown in **Figure 1**.

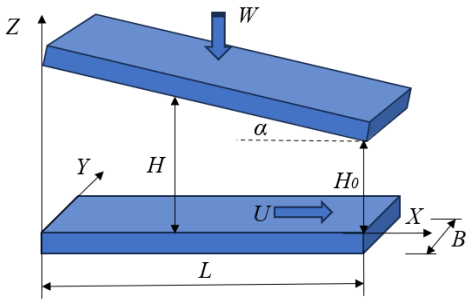

Figure 1 Slider bearing.

In a two-dimensional steady-state, the Reynolds equation for a slider bearing is expressed as:

$$\frac{\partial}{\partial x}\left(h^3\frac{\partial p}{\partial x}\right)+\frac{\partial}{\partial y}\left(h^3\frac{\partial p}{\partial y}\right)=6\eta u\frac{\partial h}{\partial x}, \qquad (1)$$

Here, h and p represent the local film thickness and pressure, respectively. The Cartesian coordinates x and y are aligned parallel and normal to the direction of sliding, respectively. The variable u denotes the relative sliding velocity between the contact surfaces, and η represents the viscosity of the lubricant.

In this study, the lubricant film thickness is considered to comprise multiscale components. The first component, denoted as $h_p(x,y)$, represents

the macroscale geometric profile of the bearing, typically ranging from 10 to 100 *μm*. The second component, $h_r(x,y)$, accounts for the microscale surface roughness including the texture of the bearing, generally in the range of 0.1 to 10 *μm*. Therefore, the total film thickness at any point *(x, y)* in the lubrication domain is expressed as:

$$h(x,y) = h_p(x,y) + h_r(x,y), \tag{2}$$

Upon determining the pressure distribution using a specific numerical method, integrating this pressure over the entire lubrication domain allows for the calculation of the load-bearing capacity, denoted by W_h.

$$W_h = \iint_\Omega p dA, \tag{3}$$

The equations were transformed using dimensionless parameters:

$$X = \frac{x}{L}, Y = \frac{y}{B}, H = \frac{h}{h_0}, P = \frac{ph_0^2}{\eta u L}, \tag{4}$$

The slider, with a length *L* and a width *B*, has its upper and lower surfaces moving along the *X*-axis at a relative velocity *U*. The dimensionless film thickness is given by

$$H(X,Y) = 1 + \frac{\alpha L}{h_0}(1-X) + H_r(X,Y), \tag{5}$$

where *α* represents the inclination angle of the slider, and h_0 is the nominal oil film thickness at the outlet. The hydrodynamic lubrication is modeled by the Reynolds equation. The oil film pressure distribution is derived by solving this equation. The dimensionless form of the Reynolds equation is

$$\frac{\partial}{\partial X}\left(H^3\frac{\partial P}{\partial X}\right) + \frac{L^2}{B^2}\frac{\partial}{\partial Y}\left(H^3\frac{\partial P}{\partial Y}\right) = 6\frac{\partial H}{\partial X}, \tag{6}$$

A Dirichlet boundary condition , where *P*=0, is applied to the boundaries of the slider.

3 MULTISCALE LUBRICATION NEURAL NETWORKS (MLNN)

3.1 MLNN architectures

The structure of a Multiscale lubrication Neural Network (MLNN) for solving the Reynolds equation with rough surface, as described by equation (6), is depicted in Fig. 2. The neural network's role is to approximate the solutions P of equation (6). Thus, P is the outputs of the neural network, while the coordinates X, Y and H serve as its inputs.

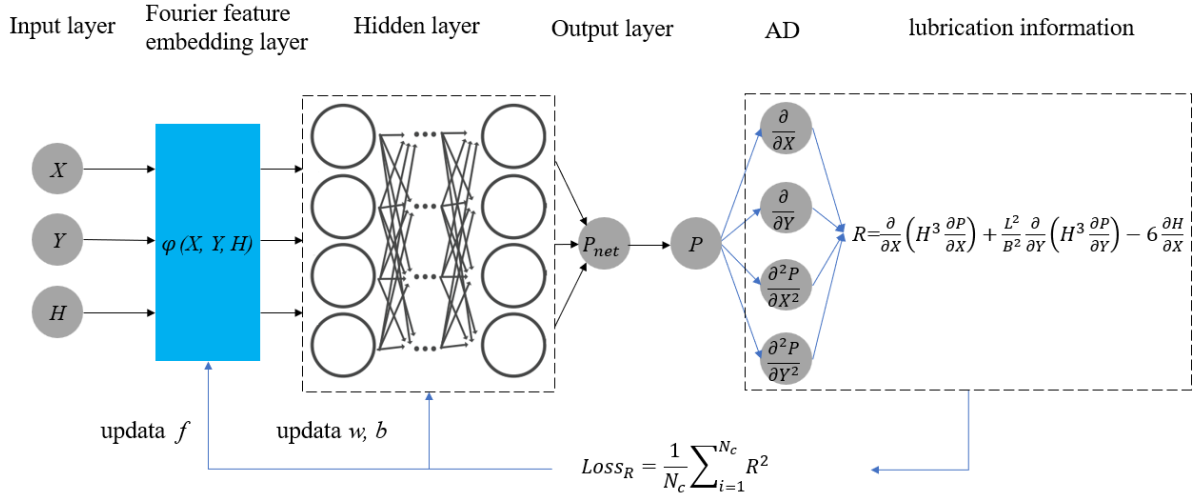

Figure 2 MLNN structure

Unlike standard physics-informed neural networks (PINNs), the proposed network architecture constructs a Fourier features network using a random features mapping as a coordinate embedding of the inputs, followed by a conventional PINN. The proposed Fourier features embedding can be viewed as a layer with trainable parameters that can be incorporated into any PINN architecture. Compared to the Fourier features network proposed by Wang et al., which uses user-specified frequencies (problem dependent and held fixed during model training), this approach allows for encoding inputs across various frequencies, enhancing the neural network's ability to learn and represent a broader spectrum of functions effectively. Once embedded, the inputs are further processed through a structure consisting of fully connected neural layers.

Mathematically, the transformation of input coordinates into Fourier feature mappings is defined as follows:

$$\varphi^i(X,Y,H) = \left[sin\left(2\pi f^i X\right); cos\left(2\pi f^i X\right); sin\left(2\pi f^i Y\right); cos\left(2\pi f^i Y\right); H\right], \quad (7)$$

For *i=1, 2, … M,* where f^i represents the frequency parameters, each sampled from a Gaussian distribution, $N(0, \sigma_i)$, with mean 0 and standard deviation σ_i. This encoding strategy significantly enhances the network's capacity to discern and model spatial hierarchies and patterns.

The subsequent processing layers are described as:

$$NN_1^i = \sigma\left(w_1\varphi^i(X,Y,H) + b_1\right), \quad for\ i = 1,2\ldots M, \quad (8)$$

$$NN_l^i = \sigma\left(w_l NN_{l-1}^i + b_l\right), \quad for\ i = 1,2\ldots M; l = 2\ldots L, \quad (9)$$

$$P_{net}(X,Y,H,w,b,f) = NN_L^i, \quad (10)$$

Here φ^i and σ represent the Fourier feature mappings and activation functions, respectively. The architecture employs weights *w* and biases *b* similar to those in a conventional fully connected neural network, with the addition of a trainable Fourier feature input encoding layer.

When training the neural network, the objective is to minimize the training error regarding prescribed boundary conditions as well as the PDE residual, $Loss = Loss_{bc} + Loss_R$.

$$Loss_{bc} = \frac{1}{N_{BC}}\sum_{i=1}^{N_{BC}}(P - P_{bc})^2 \quad (11)$$

Where P_{bc} is the pressure boundary, which is zero in this study, N_{BC} is the training data obtained through the boundary conditions, and Eq.11 ensures that the pressure boundary conditions are satisfied, representing the traditional "soft constraint" form of imposing boundary conditions. Since the boundary conditions for this paper were applied as a "hard constraint" and the loss of boundary conditions was not used for training the network.

$$Loss_R = \frac{1}{N_c}\sum_{i=1}^{N_c} R^2 \quad (12)$$

$$R = \frac{\partial}{\partial X}\left(H^3\frac{\partial \hat{P}}{\partial X}\right) + \frac{L^2}{B^2}\frac{\partial}{\partial Y}\left(H^3\frac{\partial \hat{P}}{\partial Y}\right) - 6\frac{\partial H}{\partial X} \quad (13)$$

In the formula, N_C represents the training point of the equation. By using automatic differentiation technology, the equation residual value R can be efficiently obtained.

3.2 Training of the MLNN

For networks with Fourier features, the frequency parameters were sampled from a Gaussian distribution $N(0, \sigma_i)$, where σ_i determines the frequency preference of the network's learning process. Consequently, if a network uses only one Fourier feature embedding, the convergence of the frequency components will be slower for all but the preferred frequency determined by the chosen σ_i. Therefore, it is advisable to embed the inputs using multiple Fourier feature mappings with different σ_i values to ensure that all frequency components are learned at the same rate of convergence. In this study, σ_i values were selected as 1, 20, and 50, and 30 frequency parameters were initialized from $N(0, \sigma_i)$for each value.

These mappings were then combined into a five-layer fully connected neural network, with each layer containing 100 neurons. Sigmoid activation functions were utilized within the network layers. The weights and biases of the neural network were initialized using the Glorot normal scheme. The parameters were then optimized using the ADAM optimization algorithm with an initial learning rate of 0.01 and a decay rate of 0.005 in MATLAB. Training was conducted for 1000 epochs, with a batch size of 1000. During each epoch, 1000 datasets were propagated through the neural network until all datasets had been processed, updating the network parameters accordingly. Thus, one epoch of training is equivalent to one iteration of the optimization algorithm. 60 collocation points were set up in both *x* and *y* directions within the computational domain, such that N_c = 3600.

Table 1 Setup of the MLNN and algorithm parameters

Items	value
Fourier feature embedding size	30
Hidden layers	5
Hidden layers neurons	100
Training epochs	10000
Mini batch size	1000
Initial learn rate	0.01
Decay rate	0.005

4 RESULTS

4.1 Analysis on a Randomly Textured Surface

For this analysis, a random surface was selected to represent the stochastic nature of surface roughness. The predictive performance of the

MLNN was benchmarked through a comparative evaluation against results obtained using FEM. The rough surface depicted in Figure 3 was generated using the fast Fourier transform method, with a surface roughness Ra of 0.3 μm and an autocorrelation length of 0.03 mm.

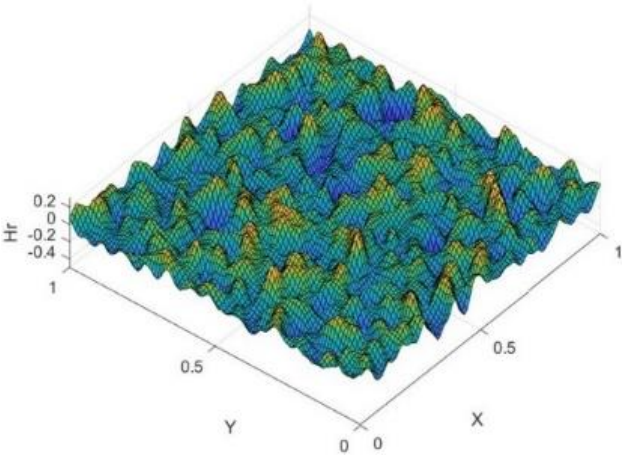

Figure 3 Rough surface for training

The pressure distributions obtained from both the FEM and the MLNN are displayed in Figure 4. The comparison reveals a close agreement between the methods, suggesting the neural network's adeptness in capturing the intricacies of the random roughness.

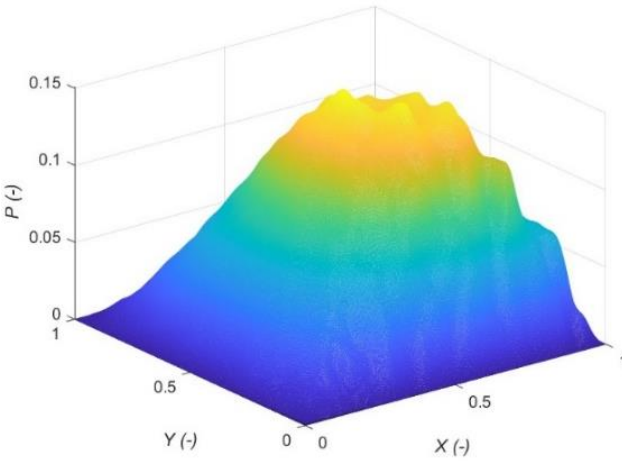

(a) FEM

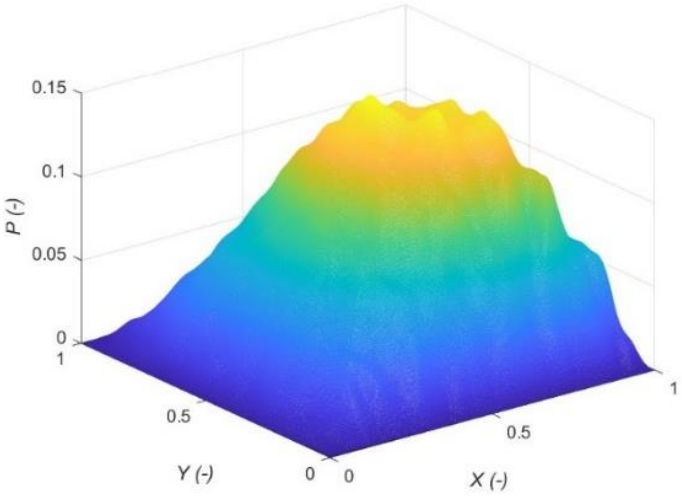

(b) MLNN

Figure 4 Pressure distributions with FEM and MLNN methods

In Figure 5 (a), the absolute error distribution between the FEM and MLNN is depicted, showing moderate discrepancies across the domain. Figure 5 (b) demonstrates the pressure distribution at a specific cross-section (Y = 0.5), where the curves from both methodologies closely align, validating the accuracy of the MLNN.

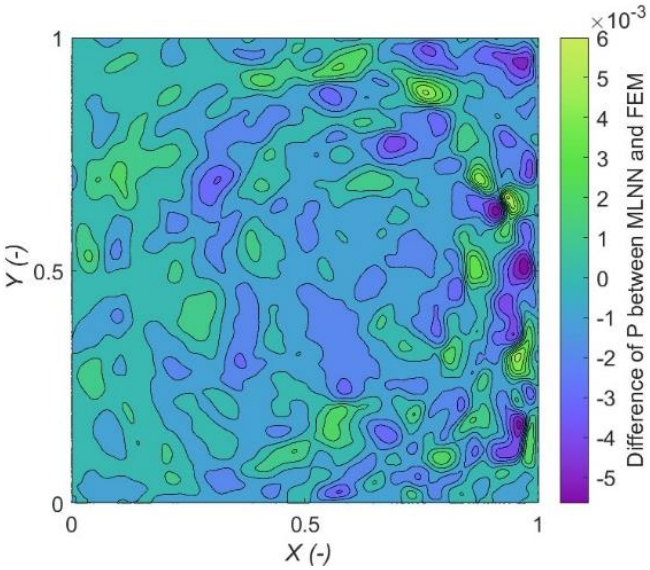

(a) absolute error

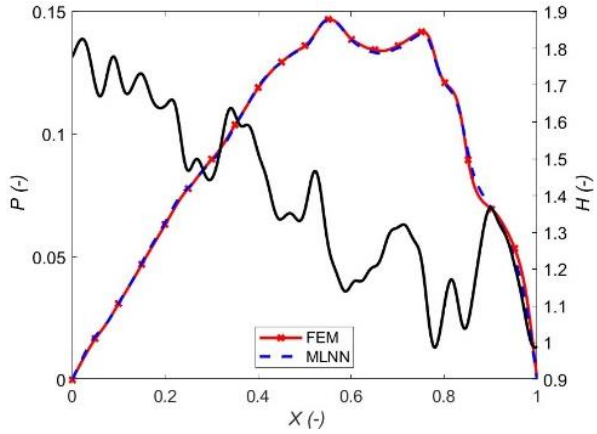

(b) pressure distribution at Y=0.5

Figure 5 Comparison of the value with FEM and MLNN methods

Table 2 provides a concise summary of the simulation outcomes, presenting the maximum pressure and load-carrying capacity assessed by both the FEM and MLNN. The disparity in maximum pressure values is nearly negligible, with MLNN results showing only a 0.33% deviation compared to FEM. Similarly, the load-carrying capacity exhibits consistency between the two methods, with an error of 0.3%.

Table 2 Comparison between FEM and MLNN

	FEM	MLNN	errors
Max. pressure	0.1505	0.15	0.33%
Load carrying capacity	0.0653	0.0651	0.3%

The examples above demonstrate that MLNN can effectively solve multiscale lubrication problems for randomly rough surfaces.

5 APPLICATION DISCUSSION

The MLNN is applicable for addressing lubrication issues related to specific surface topologies. Depending on factors such as the number of epochs, collocation points, hidden layers, and neurons per layer, training the network can take several hours. However, once trained, the problem can be resolved in seconds. One advantage of MLNN is its ability to solve multiple problems simultaneously. It can be reused for different surface topology inputs, requiring only a brief neural network evaluation that takes less than a second. This is especially advantageous in scenarios where the Reynolds equation must be repeatedly solved due to varying film thickness, such as in the computation of flow factors for rough surfaces in Figure 6. In such cases, the MLNN is notably more efficient than a conventional solver. Additionally, MLNNs are well-suited for extensive parameter studies, such as optimizing the texturing of bearing surfaces to reduce friction. This type of study involves a large number of parameters, as the texture's shape, length, width, height, arrangement, and distribution may all vary. Conducting such a parameter study with a traditional solver would be prohibitively expensive.

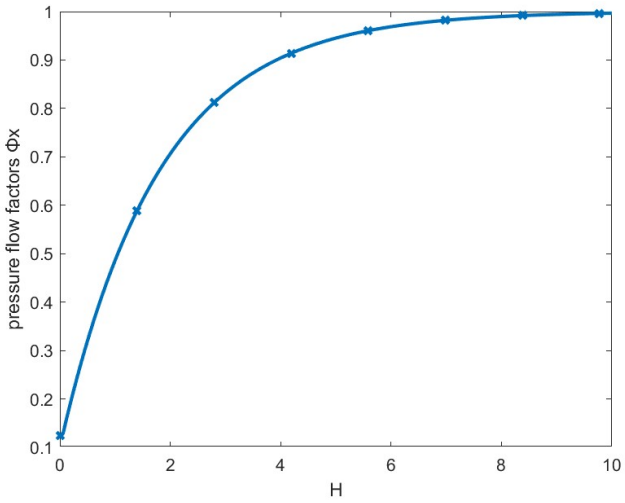

Figure 6 flow factors for rough surface

6 CONCLUSIONS

In this work, MLNN is used for the first time to solve the Reynolds equation for rough surfaces exhibiting complex multi-scale features. By integrating trainable Fourier feature embeddings into the traditional PINN architecture, this study effectively addressed the spectral bias that has hindered the thorough analysis of high-frequency surface characteristics in lubrication studies. The introduction of a multiscale lubrication neural network framework utilizing trainable Fourier features demonstrated enhanced adaptability to varying surface roughness conditions without requiring prior knowledge of the frequency distribution of the solution. This approach exhibited notable precision and efficiency in lubrication simulations, as confirmed through comparative assessments with finite element methods.

7 REFERENCES

[1] Morales-Espejel GE. Surface roughness effects in elastohydrodynamic lubrication: A review with contributions. P I Mech Eng J-J Eng, 2014, 228(11):1217-42.

[2] Gropper D, Wang L, Harvey TJ. Hydrodynamic lubrication of textured surfaces: A review of

modeling techniques and key findings. Tribol Int, 2016, 94:509-29.

[3] Patir N, Cheng HS. Application of Average Flow Model to Lubrication Between Rough Sliding Surfaces. Journal of Lubrication Technology, 1979, 101(2):220-9.

[4] Almqvist A, Essel EK, Persson LE, et al. Homogenization of the unstationary incompressible Reynolds equation. Tribol Int, 2007, 40(9):1344-50.

[5] Paturi UMR, Palakurthy ST, Reddy NS. The Role of Machine Learning in Tribology: A Systematic Review. Archives of Computational Methods in Engineering, 2023, 30(2):1345-97.

[6] Raissi M, Perdikaris P, Karniadakis GE. Physics-informed neural networks: A deep learning framework for solving forward and inverse problems involving nonlinear partial differential equations. Journal of Computational Physics, 2019, 378:686-707.

[7] Almqvist A. Fundamentals of Physics-Informed Neural Networks Applied to Solve the Reynolds Boundary Value Problem. Lubricants, 2021, 9(8):82.

[8] Li L, Li Y, Du Q, et al. ReF-nets: Physics-informed neural network for Reynolds equation of gas bearing. Computer Methods in Applied Mechanics and Engineering, 2022, 391:114524.

[9] Yadav SK, Thakre G, editors. Solution of Lubrication Problems with Deep Neural Network. Advances in Manufacturing Engineering; 2023 2023//; Singapore: Springer Nature Singapore.

[10] Zhao Y, Guo L, Wong PPL. Application of physics-informed neural network in the analysis of hydrodynamic lubrication. Friction, 2023, 11(7):1253-64.

[11] Rom M. Physics-informed neural networks for the Reynolds equation with cavitation modeling. Tribol Int, 2023, 179:108141.

[12] Xu Z-QJ. Frequency Principle: Fourier Analysis Sheds Light on Deep Neural Networks. Communications in Computational Physics, 2020, 28:1746-67.

[13] Wang S, Wang H, Perdikaris P. On the eigenvector bias of Fourier feature networks: From regression to solving multi-scale PDEs with physics-informed neural networks. Computer Methods in Applied Mechanics and Engineering, 2021, 384:113938.

[14] Etsion I. Modeling of surface texturing in hydrodynamic lubrication. Friction, 2013, 1(3):195-209.